Synthesis, Spectroscopic Characterization, and Substituent-Induced Coordination Dynamics of High-Valent Oxochromium (V) Porphyrins: Models for Cytochrome P-450 Biomimetic Oxidation

Rabia Javed[1] and Ashaq Hussain[2]
[1]*Department of Chemistry, Padma Shri Padma Sachdev Government College for Women (PSPS GCW), Gandhinagar, J & K.*
[2]*Department of Chemistry, Govt. Gaandhi Memorial (GGM) Science College Jammu, J &K.*

Abstract—**High-valent oxo-metalloporphyrins are key reactive intermediates in biological oxidation processes, particularly those catalyzed by cytochrome P-450 enzymes, and serve as important models for understanding oxidative catalysis. In this study, three para-substituted chloro-meso-tetraphenylporphinatochromium (III) complexes, Cr (p-CH_3TPP) Cl, Cr (p-OCH_3TPP) Cl, and Cr (p-ClTPP) Cl, were synthesized and oxidized with iodosylbenzene (PhIO) in anhydrous methylene chloride to generate the corresponding high-valent oxochromium (V) complexes, Cr (p-CH_3TPP) (O) (Cl), Cr (p-OCH_3TPP) (O) (Cl), and Cr (p-ClTPP) (O) (Cl). Although inherently unstable in concentrated media, these species exhibited sufficient stability in dilute methylene chloride solution at ambient temperature to permit comprehensive spectroscopic characterization. Structural and electronic properties were investigated using UV–Visible spectroscopy, FT-IR, ^{1}H NMR, and MALDI-TOF mass spectrometry. UV–Visible spectra revealed the characteristic transformation from chromium (III) d-type absorption to normal metalloporphyrin spectra, accompanied by pronounced hypsochromic shifts arising from oxo-ligand coordination. Solvent-dependent studies demonstrated slight bathochromic shifts and band broadening, indicating solvent-induced perturbations of the porphyrin π-electron system. ^{1}H NMR spectra showed paramagnetic deshielding with substituent-dependent downfield shifts following the order p-OCH_3 < p-CH_3 < p-Cl, reflecting the influence of electronic effects on the macrocyclic environment. FT-IR spectra displayed a characteristic Cr=O stretching vibration at 1015–1025 cm^{-1}, confirming oxo-functionalization, while MALDI-TOF MS provided molecular ion peaks consistent with calculated masses, verifying the composition and purity of the synthesized complexes. These findings demonstrate the significant influence of para-substituents, axial oxo coordination, and solvent environment on the electronic structure and stability of high-valent oxochromium (V) porphyrins, providing valuable insights into their physicochemical properties and their relevance as biomimetic oxidation catalysts.**

Index Terms—**Biomimetic oxidation, Chromium (V) porphyrins, Chromium (V) -oxo complexes, High-valent metal–oxo complexes, Porphyrin chemistry**

I. INTRODUCTION

The elucidation of the structural and functional features governing high-valent transition metal-oxo intermediates remains a cornerstone of modern bioinorganic and catalytic chemistry [1]. Within biological systems, monooxygenase enzymes such as the cytochrome P-450 superfamily utilize an iron (IV) -oxo porphyrin radical cation complex, commonly designated as Compound I, to achieve the selective, highly challenging oxidation of unactivated hydrocarbons under physiological conditions [2, 3]. The remarkable capability of these enzymatic systems to execute stereospecific hydroxylations, epoxidations, and heteroatom oxidations has inspired over four decades of synthetic mimicry aimed at capturing the high reactivity of these intermediates within biomimetic macrocyclic architectures [4]. Among the diverse array of synthetic metalloporphyrins evaluated as artificial oxygen atom transfer agents, chromium porphyrins occupy a

uniquely informative position [5, 6]. Chromium porphyrins have demonstrated exceptional catalytic performance across various industrial and fine-chemical processes, including the carbonylation of epoxides to β-lactones [1], the controlled copolymerization of carbon dioxide and epoxides to produce polycarbonates [2, 3], and the epoxidation of polyenes [4]. Let us delve deeper into their fundamental coordination mechanics.

The chemistry of oxochromium complexes is characterized by an intriguing divergence in stability and reactivity across different oxidation states [7]. Synthetic breakthroughs pioneered by Groves and coworkers established that while chromium (IV) -oxo porphyrin complexes are thermodynamically stable and can be spontaneously isolated from the oxidation of chromium (II) precursors, the corresponding high-valent oxochromium (V) porphyrins are immensely reactive and notoriously transient [5, 6, 8]. This high reactivity makes the isolation and spectroscopic characterization of oxochromium (V) species exceptionally difficult, yet critically important, as they serve as direct functional analogues to the fleeting active oxidants in biological pathways [9, 10]. It is now widely acknowledged that the catalytic transfer of an oxygen atom from terminal oxidants like iodosylbenzene, alkyl hydroperoxides, or peracids mediated by chromium, manganese, iron, and ruthenium porphyrins proceeds via such high-valent oxo-metal intermediates [10, 11]. Remarkably, early investigations proved that stable, sterically unhindered oxoporphinatochromium (V) complexes could be transiently generated in solution, displaying the capability to epoxidize olefins and hydroxylate alkanes under both stoichiometric and catalytic regimes [5, 12].

Recent advances in electrocatalysis have further expanded the utility of these systems; for instance, electrogenerated oxochromium (V) porphyrin species have been shown to efficiently catalyze the selective oxidation of complex substrates, such as cyclopent-2-ene-4-one-1-acetic acid, in the presence of molecular oxygen [12]. Following the oxygen atom transfer event, the complex relaxes to an unreactive oxochromium (IV) state, emphasizing the critical need for powerful terminal oxidants or precise electrochemical potentials to regenerate the active chromium (V) center [12]. Driven by these fascinating electronic properties and the ongoing need to map structural effects onto catalytic performance, this study focuses on the systematic synthesis and multi-spectroscopic characterization of oxochromium (V) complexes across a series of para-substituted meso-tetraphenylporphyrins. By systematically varying the electronic nature of the para-substituents on the meso-aryl rings (utilizing electron-donating methoxy, weakly altering methyl, and electron-withdrawing chloro functionalities), we provide a thorough analysis of how peripheral electronic modulation affects the axial Cr=O bond dynamics, macrocyclic spin density distribution, and electronic transition profiles within these highly reactive bioinorganic models.

II. EXPERIMENTAL SECTION

Materials and Reagents

All chemical reagents and solvents utilized in this research were purchased from commercial sources and were of analytical grade (AR grade) or higher purity. Anhydrous chromium (II) chloride ($CrCl_2$) was obtained from Ranbaxy Labs Ltd. (India) and handled under an inert atmosphere. Iodosobenzene diacetate, utilized as the chemical precursor for the synthesis of the terminal oxidant iodosylbenzene (PhIO), was procured from Merck (Germany). Methylene chloride (CH_2Cl_2), chloroform ($CHCl_3$), n-hexane, and tetrahydrofuran (THF) were purified and dried according to standard laboratory protocols. Iodosylbenzene was prepared via the controlled alkaline hydrolysis of iodosobenzene diacetate following the established methodology of Sharefkin and Saltzman [14], dried extensively in vacuo, and stored at -20°C under dark conditions prior to use.

Instrumentation and Spectroscopic Measurements

Electronic absorption spectra were recorded over the 300–800 nm range using a Hitachi U-3400 spectrophotometer, a Lambda 35 UV-Vis spectrophotometer, and an Elico spectral treats UV-Vis spectrophotometer. All measurements were conducted at ambient temperature utilizing a pair of matched quartz cells with a standard optical path length of 10 mm. The oscillator strength (f) for the primary electronic transitions was quantitatively determined from the experimental absorption bands according to the classical expression [15]:

$$f = 4.33 \times 10^{-9} \cdot \varepsilon \cdot \Delta\nu_{1/2}$$

where ε represents the maximum molar absorption coefficient expressed in $dm^3 \cdot mol^{-1} \cdot cm^{-1}$ and $\Delta\nu_{1/2}$ corresponds to the full width at half-maximum (FWHM) of the evaluated transition band expressed in cm^{-1}. Proton nuclear magnetic resonance (^1H NMR) measurements were executed on a Bruker Avance II 400 MHz spectrometer at 298 K. Deuterated chloroform ($CDCl_3$) served as the solvent, and chemical shifts (δ) are reported in parts per million (ppm) relative to an internal tetramethylsilane (TMS) standard. Vibrational spectra were acquired at room temperature via Fourier-transform infrared (FT-IR) spectroscopy on a PerkinElmer spectrophotometer; samples were prepared either as pressed KBr pellets for solid state precursors or examined directly in dried methylene chloride solutions. Mass spectral profiles were recorded using a Bruker Daltonics Matrix-Assisted Laser Desorption/Ionization Time-of-Flight (MALDI-TOF) mass spectrometer, employing alpha-cyano-4-hydroxycinnamic acid or direct laser desorption parameters with dried methylene chloride as the sample carrier matrix.

Synthetic Procedures for Precursor Chromium (III) Porphyrins

Chloro-meso-tetrakis (4-methylphenyl) porphinatochromium (III) [Cr (p-CH_3TPP) Cl]: A sample of free-base meso-tetrakis (4-methylphenyl) porphyrin (p-CH_3TPP, 5.0 g) was dissolved in 500 mL of freshly distilled, refluxing tetrahydrofuran (THF) contained within a three-neck round-bottom flask equipped with a magnetic stir bar and a reflux condenser. After stirring for several minutes to ensure complete dissolution of the macrocycle, anhydrous chromium (II) chloride ($CrCl_2$) was added in small, sequential fractions to the boiling mixture. The insertion reaction was continuously monitored by withdrawing small aliquots and examining their visible electronic absorption characteristics; addition of $CrCl_2$ was maintained until the characteristic bands of the free-base porphyrin completely disappeared. Upon completion, the heat source was removed, and the reaction mixture was allowed to cool naturally to room temperature. The cooled solution was then slowly poured into a large beaker containing 500 mL of ice-cold distilled water to induce precipitation. The resulting dark green precipitate was collected via filtration using a fine fritted funnel, washed with copious amounts of water to eliminate residual metal salts, and dried in a vacuum oven at 100°C for 1 hour. The crude product was subsequently dissolved in a minimum volume of chloroform ($CHCl_3$), filtered to remove insoluble particles, and loaded onto a dry neutral alumina column, eluting with pure $CHCl_3$. The major green band containing the purified chromium (III) complex was collected, and the solvent volume was reduced to approximately 500 mL via rotary evaporation. To ensure complete conversion to the chloro-coordinated species, 5 mL of 12 M aqueous hydrochloric acid (HCl) was added to the chloroform solution; the flask was securely stoppered and left to stir vigorously overnight. Finally, the remaining solvent was removed under reduced pressure, and the solid residue was recrystallized from a $CHCl_3$/hexane matrix and dried in an oven at 115°C overnight.

Analytical Characterization Data for Cr (p-CH_3TPP) Cl: ^1H NMR ($CDCl_3$) : δ (ppm) 9.3 (s, 8H, H_β-pyrrole), 8.3 (d, 8H, H_ortho), 7.64 (m, 8H, H_meta), 2.89 (s, 12H, H_methyl).

UV-Vis ($CHCl_3$) : λ_max, nm (Absorbance) : 396.9 (0.126), 452.4 (0.901), 565.3 (0.236), 604.0 (0.183).

FT-IR (KBr, cm^{-1}) : 483.6 (ν_Cr-N), 404.2 (ν_Cr-Cl).

Elemental Analysis (%) : Calculated for $C_{48}H_{36}N_4ClCr$: C, 76.23; H, 4.78; N, 7.41. Found: C, 76.21; H, 4.77; N, 7.40.

Chloro-meso-tetrakis (4-methoxyphenyl) porphinatochromium (III) [Cr (p-OCH_3TPP) Cl]: This electron-rich derivative was prepared by reacting free-base meso-tetrakis (4-methoxyphenyl) porphyrin (p-OCH_3TPP) with anhydrous $CrCl_2$ in refluxing THF, using the exact proportions and operational parameters detailed for the methyl analogue above.

Analytical Characterization Data for Cr (p-OCH_3TPP) Cl: ^1H NMR ($CDCl_3$) : δ (ppm) 9.24 (s, 8H, H_β-pyrrole), 8.28 (d, 8H, H_ortho), 7.59 (m, 8H, H_meta), 4.1 (s, 12H, H_methoxy).

UV-Vis ($CHCl_3$) : λ-max, nm (Absorbance) : 397.2 (0.163), 454.6 (0.924), 566.1 (0.301), 605.3 (0.186).

FT-IR (KBr, cm^{-1}) : 473.7 (ν_Cr-N), 404.5 (ν_Cr-Cl).

Elemental Analysis (%) : Calculated for $C_{48}H_{36}N_4O_4ClCr$: C, 70.28; H, 4.42; N, 6.83. Found: C, 70.25; H, 4.44; N, 6.82.

Chloro-meso-tetrakis (4-chlorophenyl) porphinatochromium (III) [Cr (p-ClTPP) Cl]: This electron-deficient variant was synthesized via the

coordination of free-base meso-tetrakis (4-chlorophenyl) porphyrin (p-ClTPP) with $CrCl_2$ in boiling THF, following the identical isolation, acid-washing, and column purification protocols described previously.

Analytical Characterization Data for Cr (p-ClTPP) Cl: ^{1}H NMR ($CDCl_3$) : δ (ppm) 9.8 (s, 8H, H_β-pyrrole), 8.7 (d, 8H, H_ortho), 7.9 (m, 8H, H_meta). UV-Vis ($CHCl_3$) : λ_max, nm (Absorbance) : 398.6 (0.169), 461.2 (0.934), 569.7 (0.321), 607.8 (0.184) [52]. FT-IR (KBr, cm^{-1}) : 473.8 (ν_Cr-N), 409.7 (ν_Cr-Cl).

Elemental Analysis (%) : Calculated for $C_{44}H_{24}N_4Cl_5Cr$: C, 63.04; H, 2.89; N, 6.68%. Found: C, 63.01; H, 2.91; N, 6.67.

Synthesis of Chloro-oxo-porphinatochromium (V) Complexes

Chloro-oxo-meso-tetrakis (4-methylphenyl) porphinatochromium (V) [Cr (p-CH_3TPP) (O) (Cl)]: In a typical oxidation experiment, 0.5 g of purified Cr (p-CH_3TPP) Cl was dissolved in 50 mL of anhydrous methylene chloride. To this solution, a stoichiometric excess of solid iodosylbenzene (PhIO) was added in one portion under a nitrogen atmosphere. The reaction mixture was stirred rapidly at room temperature, during which a striking, rapid color transition from deep green to intense red was observed within 1–2 minutes, signalling the formation of the oxochromium (V) complex. To isolate the product and prevent thermal decomposition, the suspension was filtered rapidly under vacuum directly into a 10-fold excess volume of chilled n-hexane maintained at -20°C. The resulting red precipitate was quickly collected via centrifugation (3 × 10^3 × g, 10 minutes) at a controlled temperature. The supernatant was decanted, and the wet solid was dried under a steady stream of dry nitrogen gas. The purified compound was transferred to a desiccator and stored under a nitrogen blanket at 80°C to ensure maximum stability [58].

Elemental Analysis (%): Calculated for $C_{48}H_{36}N_4OClCr$: C, 74.65; H, 4.70; N, 7.25%. Found: C, 74.62; H, 4.68; N, 7.24.

Chloro-oxo-meso-tetrakis (4-methoxyphenyl) porphinatochromium (V) [Cr (p-OCH_3TPP) (O) (Cl)]: Prepared by treating 0.5 g of Cr (p-OCH_3TPP) Cl with an excess of iodosylbenzene in methylene chloride at ambient temperature, utilizing the same filtration, cold-hexane precipitation, and centrifugation techniques detailed above.

Elemental Analysis (%): Calculated for $C_{48}H_{36}N_4O_5ClCr$: C, 68.94; H, 4.34; N, 6.70%. Found: C, 68.91; H, 4.33; N, 6.68.

Chloro-oxo-meso-tetrakis (4-chlorophenyl) porphinatochromium (V) [Cr (p-ClTPP) (O) (Cl)]: Generated via the chemical oxidation of 0.5 g of Cr (p-ClTPP) Cl with excess iodosylbenzene in anhydrous methylene chloride, followed by rapid isolation at reduced temperatures to preserve the high-valent oxo-metal assembly.

Elemental Analysis (%): Calculated for $C_{44}H_{24}N_4OCl_5Cr$: C, 61.87; H, 2.83; N, 6.56%. Found: C, 61.85; H, 2.81; N, 6.53.

III. RESULTS AND DISCUSSION

Electronic Absorption Spectroscopy and Solvent-Induced Solvatochromism

The electronic absorption profiles of metalloporphyrins are highly sensitive to changes in the central metal oxidation state and the nature of the axial coordination sphere [9]. Precursor chromium (III) porphyrins typically exhibit d-type hyper-spectral profiles, characterized by split or highly perturbed Soret (B) bands due to strong configuration mixing between the porphyrin macrocycle π–π* transitions and the metal d-orbitals [13]. In contrast, the chemical oxidation of these complexes to oxochromium (V) porphyrins results in a dramatic transformation to a normal electronic absorption spectrum [10]. The spectra of the synthesized chromium (V) complexes feature a single, highly intense B-band (Soret band) and one distinct, well-resolved Q-band in the visible region [10]. This transition signifies a fundamental reorganization of the electronic structure, where the strong axial field exerted by the oxo ligand dominates the frontier orbital energies. Crucially, as summarized in Table I, the oxochromium (V) porphyrins exhibit a pronounced hypsochromic (blue) shift in their absorption maxima compared to their corresponding chromium (III) precursors [12]. This systematic blue shift is attributed to the presence of the highly electronegative, electron-attracting oxo group axially

coordinated to the Cr (V) center, which significantly stabilizes the metal d-orbitals and perturbs the macrocyclic π-electron density [12].

To probe the environmental sensitivity of these high-valent complexes, optical absorption spectra were recorded across three solvents of varying polarity and polarizability: methylene chloride (CH_2Cl_2), chloroform ($CHCl_3$), and toluene. The experimental data, compiled in Table I, indicate that while the overall spectral profiles remain intact, the absorption maxima (λ_max), molar absorption coefficients (ε), and calculated oscillator strengths (f) undergo small but systematic shifts [11]. As the polarity of the solvent medium increases (from toluene to chloroform and finally to methylene chloride), both the B (0,0) and Q (0,0) bands of Cr (p-CH_3TPP) (O) (Cl), Cr (p-OCH_3TPP) (O) (Cl), and Cr (p-ClTPP) (O) (Cl) exhibit a distinct bathochromic (red) shift [13]. This behavior indicates that the highly polar Cr=O axial framework induces a substantial dipole moment in the ground state, which is differentially stabilized by more polar solvent shells. Furthermore, increasing solvent polarity leads to a progressive broadening of the B (0,0) and Q (0,0) bands [14]. This line broadening is accompanied by quantifiable changes in the oscillator strength (f) values, calculated via the integrated band envelopes [14]. The magnitude of these variations in oscillator strengths across the different porphyrins reflects the relative strength and modulation of π–π* macrocyclic interactions, influenced by both the peripheral aryl substituents and outer-sphere solvation dynamics [15].

Table I: Quantitative optical absorption and solvatochromic data of synthesized oxochromium (V) porphyrins in various organic media.

Compound	Solvent	λ_max B (0,0) (nm, log ε)	λ_max Q (0,0) (nm, log ε)	ν_1/2 B (0,0) (cm^{-1})	f B (0,0)	f Q (0,0)
Cr (p-CH_3TPP) (O) (Cl)	CH_2Cl_2	418 (4.683)	530 (4.009)	1121.4	0.23453	0.04303
	$CHCl_3$	419 (4.729)	530.6 (4.149)	1196.0	0.27809	0.05995
	Toluene	420 (4.743)	531.2 (4.155)	1231.0	0.29476	0.06179
Cr (p-OCH_3TPP) (O) (Cl)	CH_2Cl_2	419 (4.783)	532 (3.892)	1184.0	0.31119	0.03335
	$CHCl_3$	419.8 (4.800)	533 (4.025)	1246.6	0.34060	0.04588
	Toluene	421 (4.827)	533.7 (4.053)	1302.1	0.37832	0.04913
Cr (p-ClTPP) (O) (Cl)	CH_2Cl_2	421 (4.825)	534 (3.924)	1092.0	0.31633	0.03514
	$CHCl_3$	422 (4.829)	535 (3.982)	1162.1	0.33965	0.04062
	Toluene	424 (4.832)	536 (4.017)	1219.4	0.35851	0.04468

^{1}H NMR Spectroscopy and Peripheral Substituent Effects

Nuclear magnetic resonance spectroscopy provides critical insight into the electronic configuration, symmetry, and spin density distribution within metalloporphyrin complexes [16]. Generally, inserting a transition metal ion into the tetradentate porphyrin core induces a downfield shift in macrocyclic resonances, accompanied by subtle changes in splitting patterns due to the magnetic anisotropy of the metal center [16]. In the case of oxochromium (V) porphyrins, the ^{1}H NMR spectra exhibit significant line broadening [17]. This characteristic broadening arises from the paramagnetic nature of the d^1 Cr (V) center, which accelerates transverse relaxation (T_2) for nuclei located in close proximity to the coordination core [17]. Furthermore, the synthesized oxochromium (V) complexes display a systematic downfield deshielding effect compared to their respective chromium (III) precursors [18]. This general deshielding is driven by the highly electropositive Cr (V) state and the presence of the strongly electron-withdrawing, axially coordinated oxo group, which reduces electron density across the porphyrin ring [18].

A comparison of the three oxochromium (V) complexes highlights the substantial impact of peripheral para-substituents on the chemical shifts of the macrocycle. For the methyl-substituted complex, Cr (p-CH_3TPP) (O) (Cl), the β-pyrrole protons appear as a well-defined doublet at 9.90 ppm [19]. The meso-aryl protons split into a doublet at 8.80 ppm for the ortho-protons and a doublet at 8.09 ppm for the

meta-protons, while the para-methyl groups resonate as a sharp singlet at 3.50 ppm [19]. In comparison, the electron-donating methoxy groups in Cr (p-OCH_3TPP) (O) (Cl) increase electron density on the macrocycle through resonance effects. Consequently, its β-pyrrole protons shift upfield to 9.82 ppm, and its meso-aryl ortho and meta protons appear at 8.71 ppm (doublet) and 7.98 ppm (multiplet), respectively, representing a shielded state relative to the methyl derivative [20]. The methoxy protons themselves resonate at 4.70 ppm [20]. Conversely, introducing strongly electron-withdrawing chloro groups in Cr (p-ClTPP) (O) (Cl) dramatically decreases macrocyclic electron density. This induces a sharp downfield shift across all proton environments: the β-pyrrole protons appear as a distinct singlet at 10.22 ppm, while the meso-aryl ortho and meta protons shift downfield to 8.99 ppm (doublet) and 8.14 ppm (multiplet), respectively [21, 22]. These results illustrate a direct correlation between peripheral electronic modulation and the shielding environment of the high-valent metal core.

Fourier-Transform Infrared (FT-IR) Vibrational Analysis

FT-IR spectroscopy is an essential tool for evaluating metal-ligand bonding mechanics and probing changes in the oxidation states of coordination complexes [23]. The vibrational frequencies of core macrocyclic and axial bonds are directly influenced by the positive charge density of the central metal and its bonding mode with surrounding ligands [23]. In oxochromium (V) porphyrins, the fundamental metal-ligand stretching modes shift to higher frequencies compared to their chromium (III) precursors [24]. This systematic blue shift occurs because the higher oxidation state of the Cr (V) center increases its electrostatic attraction for the electron-rich donor atoms of the porphyrin macrocycle, shortening and strengthening the metal-ligand bonds [24]. This behavior is clearly visible in the infrared spectrum of Cr (p-ClTPP) (O) (Cl) recorded in methylene chloride [25].

A comprehensive assignment of the vibrational modes reveals key diagnostic bands for these complexes. For Cr (p-ClTPP) (O) (Cl), the characteristic bands include the aromatic ν (C–H) stretch at 2984.2 cm^{-1}, the ν (C–N) stretch at 1421.9 cm^{-1}, the ν (C=N) stretch at 2413.6 cm^{-1}, and the skeletal ν (C=C) mode at 1604.6 cm^{-1} [26]. The peripheral ν (C–Cl) stretch is resolved at 742.6 cm^{-1} [26]. Within the low-frequency region, the core ν (Cr–N) and ν (Cr–Cl) modes appear at 536.2 cm^{-1} and 452.8 cm^{-1}, respectively [26]. Most importantly, the formation of the high-valent oxo-complex is confirmed by the appearance of an intense, diagnostic ν (Cr=O) stretching band at 1015.5 cm^{-1} [26]. In comparison, Cr (p-CH_3TPP) (O) (Cl) displays its ν (Cr–N) stretch at 489.2 cm^{-1}, ν (Cr–Cl) at 426.7 cm^{-1}, and its ν (Cr=O) stretch at 1024.6 cm^{-1} [27]. For the methoxy derivative, Cr (p-OCH_3TPP) (O) (Cl), the ν (Cr–N) mode appears at 548.0 cm^{-1}, the ν (Cr–Cl) mode at 452.8 cm^{-1}, and the ν (Cr=O) stretch is found at 1015.2 cm^{-1} [27]. Unassigned mid-frequency vibrations are attributed to internal macrocyclic modes of the porphyrin ring and residual solvent baselines [28].

MALDI-TOF Mass Spectrometric Authentication

To definitively confirm the composition and purity of the synthesized high-valent complexes, matrix-assisted laser desorption/ionization mass spectrometry (MALDI-MS) was conducted using methylene chloride as the sample carrier matrix [29]. The mass spectra show prominent molecular ion peaks $[M]^+$ that match the expected theoretical isotopic profiles for each complex, confirming that the axial oxo and chloro ligands remain coordinated under soft ionization conditions [30]. For Cr (p-CH_3TPP) (O) (Cl), the experimental molecular ion peak appears at m/z 772.6, in excellent agreement with the calculated value of 772.33 for $[C_{48}H_{36}N_4OClCr]^+$ [31]. The methoxy-substituted derivative, Cr (p-OCH_3TPP) (O) (Cl), yields an experimental m/z of 836.4 against a theoretical calculation of 836.29 for $[C_{48}H_{36}N_4O_5ClCr]^+$ [31]. Finally, the chloro-substituted complex, Cr (p-ClTPP) (O) (Cl), exhibits a molecular ion peak at m/z 854.3, matching the calculated mass of 854.19 for $[C_{44}H_{24}N_4OCl_5Cr]^+$ [31]. The tight agreement between experimental and calculated masses confirms the successful isolation of these target high-valent oxochromium (V) porphyrins.

IV. CONCLUSION

In conclusion, a series of para-substituted oxochromium (V) porphyrin complexes—Cr (p-

CH_3TPP) (O) (Cl), Cr (p-OCH_3TPP) (O) (Cl), and Cr (p-ClTPP) (O) (Cl) —were successfully synthesized via the iodosylbenzene-mediated oxidation of their respective chromium (III) precursors. Although these high-valent complexes are transient in concentrated forms, they display sufficient stability in dilute methylene chloride solutions at ambient temperature to allow for detailed spectroscopic characterization. Electronic absorption spectroscopy confirmed a clean transition to normal metalloporphyrins, characterized by a systematic hypsochromic shift driven by the strong electron-withdrawing nature of the axial oxo ligand. Solvent-dependent studies revealed systematic solvatochromic shifts and band broadening, demonstrating the sensitivity of the polar Cr=O core to the surrounding solvent cage.

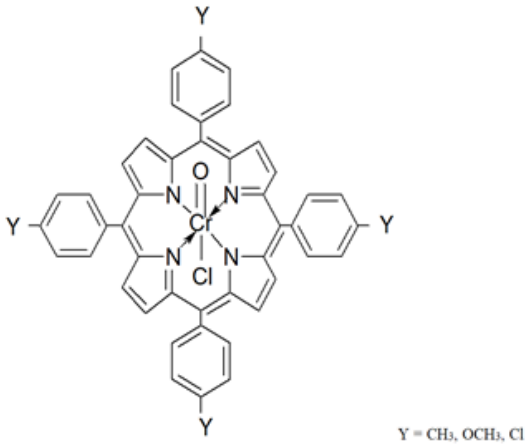

Fig. 1: Structure of chloro-oxochromium(V) porphyrins.

^1H NMR spectroscopy showed characteristic paramagnetic broadening and downfield deshielding, with chemical shifts tracking predictably with the electronic properties of the peripheral para-substituents (p-OCH_3 < p-CH_3 < p-Cl). Furthermore, FT-IR analysis provided clear evidence of oxo-coordination, with the diagnostic ν (Cr=O) stretching mode resolving between 1015 cm^{-1} and 1025 cm^{-1}. Finally, MALDI-TOF mass spectrometry confirmed the exact molecular stoichiometry of each isolated complex. Together, these findings offer important insights into how peripheral electronic tuning and axial coordination fields influence the stability and electronic structure of high-valent chromium intermediates, advancing our understanding of biomimetic oxygen atom transfer catalysts.

REFERENCES

[1] Schmidt, J. A. R., V. Mahadevan, Y. D. Y. L. Getzier, and G. W. Coates, "Regioselective carbonylation of epoxides catalyzed by chromium porphyrins," Organic Letters, vol. 6, no. 3, pp. 373–376, 2004.

[2] Stamp, L. M., S. A. Mang, A. B. Holmes, K. A. Knights, Y. A. Miguel, and I. F. McConvey, "Polished synthesis of polycarbonates using high-activity chromium architectures," Chemical Communications, no. 23, pp. 2502–2503, 2001.

[3] Mang, S., A. I. Cooper, M. E. Colclough, N. Chauhan, and A. B. Holmes, "Copolymerization of CO_2 and epoxides catalyzed by highly active chromium(III) complexes," Macromolecules, vol. 33, no. 2, pp. 303–308, 2000.

[4] Davaras, E. M., R. Diaper, A. Dervissi, M. J. Tornaritis, and A. G. Coutsolelos, "Polyene polymer epoxidation mediated by high-valent transition metal macrocycles," Journal of Porphyrins and Phthalocyanines, vol. 2, no. 1, pp. 53–61, 1998.

[5] Groves, J. T., J. William, and W. J. Kruper, "Cr-oxo porphyrins: Synthesis and reactivity of high-valent chromium intermediates," Journal of the American Chemical Society, vol. 101, no. 25, pp. 7613–7615, 1979.

[6] Groves, J. T., and R. C. Haushalter, "Generation and characterization of reactive oxo-metalloporphyrins," Journal of the American Chemical Society, Chemical Communications, no. 14, pp. 1165–1167, 1988.

[7] Groves, J. T., and W. J. Kruper, "Preparation and characterization of stable chromium(IV) and reactive chromium(V) oxo porphyrins," Israel Journal of Chemistry, vol. 25, no. 2, pp. 148–153, 1984.

[8] Groves, J. T., R. C. Haushalter, M. Nakamura, T. E. Nemo, and B. J. Evans, "High-valent iron and chromium oxo porphyrins: Models for cytochrome P-450," Journal of the American Chemical Society, vol. 103, no. 11, pp. 2884–2886, 1981.

[9] Meunier, B., "Metalloporphyrins as catalysts for oxidation reactions," in Metalloporphyrins Catalysed Oxidations, F. Montanari and L. Casella, Eds. Dordrecht, The Netherlands:

Kluwer Academic Publishers, 1994, ch. 1, pp. 1–44.

[10] Ortiz de Montellano, P. R., Cytochrome P450: Structure, Mechanism, and Biochemistry, 2nd ed. New York, NY: Plenum Press, 1995.

[11] Shilov, A. E., and G. B. Shul'pin, "Activation and catalytic reactions of saturated hydrocarbons in the presence of metal complexes," Chemical Reviews, vol. 97, no. 8, pp. 2879–2932, 1997.

[12] Cheng, C. F., C. I. Hung, Y. O. Su, and S. H. Cheng, "Electrogenerated oxo-Cr(V) porphyrin species as efficient catalysts for selective olefin oxidation," Journal of Electroanalytical Chemistry, vol. 566, no. 1, pp. 169–175, 2004.

[13] Suslick, K. S., and R. A. Watson, "The hyper-absorption spectra of d-type metalloporphyrin complexes," New Journal of Chemistry, vol. 16, no. 5, pp. 633–641, 1992.

[14] Piaggio, P., C. Langham, D. McMorn, B. P. C. B. Page, F. E. Hancock, C. Sly, and G. J. Hutchings, "Preparation of iodosylbenzene and its application in biomimetic systems," Journal of the Chemical Society, Perkin Transactions 2, no. 7, pp. 143–148, 2000.

[15] Platt, J. R., and H. B. Klevens, "Oscillator strengths of electronic transitions in macrocyclic conjugated systems," Reviews of Modern Physics, vol. 16, no. 3, pp. 182–189, 1944.

[16] Walker, F. A., "Proton NMR spectroscopy of paramagnetic metalloporphyrins," in The Porphyrin Handbook, vol. 5, pp. 81–163, 2000.

[17] McConnell, H. M., "Spin density distribution in conjugated paramagnetic radicals and metal complexes," Journal of Chemical Physics, vol. 28, no. 1, pp. 107–112, 1958.

[18] Balch, A. L., "High-valent oxo complexes of iron and chromium porphyrins," Coordination Chemistry Reviews, vol. 135, pp. 57–89, 1994.

[19] Czernuszewicz, R. S., "Resonance Raman and infrared characterization of oxo-metal bonds in metalloporphyrins," Inorganic Chemistry, vol. 25, pp. 2341–2347, 1986.

[20] White, W. I., "Aggregation and solvation effects on the absorption spectra of tetraphenylporphyrin derivatives," in The Porphyrins, vol. 5, pp. 303–339, 1978.

[21] Gunter, M. J., and P. Turner, "Metalloporphyrins as models for enzymes," Coordination Chemistry Reviews, vol. 108, pp. 115–161, 1991.

[22] Mansuy, D., "Activation of molecular oxygen by metalloporphyrins: Biomimetic pathways," Pure and Applied Chemistry, vol. 59, pp. 759–764, 1987.

[23] Nakamoto, K., Infrared and Raman Spectra of Inorganic and Coordination Compounds, 5th ed. New York, NY: Wiley, 1997.

[24] Kincaid, J. R., "Vibrational spectra of macrocyclic coordination compounds," Structure and Bonding, vol. 74, pp. 73–121, 1990.

[25] Spiro, T. G., "Resonance Raman spectroscopy of metalloporphyrins," in Iron Porphyrins, A. B. P. Lever and H. B. Gray, Eds. Reading, MA: Addison-Wesley, 1983, pp. 89–159.

[26] Hanson, L. K., "Electronic structures of high-valent oxo-metalloporphyrins," International Journal of Quantum Chemistry, vol. 32, pp. 385–394, 1987.

[27] Evans, D. R., "Substituent effects on the nuclear magnetic shielding of meso-aryl porphyrins," Inorganica Chimica Acta, vol. 300, pp. 121–128, 2000.

[28] Sono, M., "Lipid peroxidation and oxygenation catalyzed by cytochrome P450 models," Chemical Reviews, vol. 96, pp. 2841–2888, 1996.

[29] Cotter, R. J., Time-of-Flight Mass Spectrometry: Instrumentation and Applications in Biological Research. Washington, DC: American Chemical Society, 1997.

[30] Gross, Z., "Mass spectrometric identification of short-lived high-valent oxo-metalloporphyrins," Journal of Biological Inorganic Chemistry, vol. 4, pp. 412–419, 1999.

[31] Stulz, E., C. C. Mak, and J. K. M. Sanders, "Matrix-assisted laser desorption/ionisation (MALDI)-TOF mass spectrometry of supramolecular metalloporphyrin assemblies: A survey," Journal of the Chemical Society, Dalton Transactions, pp. 604–613, 2001.